METHODS AND APPLICATIONS

Biolayer interferometry of lipid nanodisc-reconstituted yeast vacuolar H^+-ATPase

Stuti Sharma and Stephan Wilkens*

Department of Biochemistry and Molecular Biology, SUNY Upstate Medical University 750 East Adams Street, Syracuse, New York 13210

Received 22 December 2016; Accepted 17 February 2017
DOI: 10.1002/pro.3143
Published online 27 February 2017 proteinscience.org

Abstract: Vacuolar H^+-ATPase (V-ATPase) is a large, multisubunit membrane protein complex responsible for the acidification of subcellular compartments and the extracellular space. V-ATPase activity is regulated by reversible disassembly, resulting in cytosolic V_1-ATPase and membrane-integral V_0 proton channel sectors. Reversible disassembly is accompanied by transient interaction with cellular factors and assembly chaperones. Quantifying protein-protein interactions involving membrane proteins, however, is challenging. Here we present a novel method to determine kinetic constants of membrane protein–protein interactions using biolayer interferometry (BLI). Yeast vacuoles are solubilized, vacuolar proteins are reconstituted into lipid nanodiscs with native vacuolar lipids and biotinylated membrane scaffold protein (MSP) followed by affinity purification of nanodisc-reconstituted V-ATPase (V_1V_0ND). We show that V_1V_0ND can be immobilized on streptavidin-coated BLI sensors to quantitate binding of a pathogen derived inhibitor and to measure the kinetics of nucleotide dependent enzyme dissociation.

Keywords: vacuolar ATPase; lipid nanodiscs; biolayer interferometry; protein–protein interaction; inhibitor binding; membrane protein

Introduction

The vacuolar H^+-ATPase (V-ATPase; V_1V_0-ATPase) is an ATP-dependent proton pump present in all eukaryotic cells. The enzyme is typically localized to the endomembrane system and functions in acidifying organelles for essential cellular functions including pH homeostasis, membrane trafficking, endocytosis, hormone secretion, and lysosomal degradation.[1] In certain specialized cell types such as osteoclasts, renal tubular cells and cells of the male reproductive tract, the V-ATPase is found on the plasma membrane where it acidifies the extracellular environment. Complete loss of V-ATPase activity is embryonic lethal in mammals,[2,3] highlighting the essential nature of the enzyme. Not surprisingly therefore, aberrant V-ATPase displaying hyper- or hypo-activity has been implicated in a number of widespread human diseases

Abbreviations: BLI, biolayer interferometry; ConA, concanamycin A; MSP, membrane scaffold protein; V-ATPase, vacuolar ATPase; V_1V_0ND, lipid nanodisc reconstituted vacuolar ATPase.

Additional Supporting Information may be found in the online version of this article.

Narrative: The enzymatic activity of the proton pumping vacuolar ATPase (V-ATPase) is regulated by reversible disassembly *in vivo*, a process that can be exploited for therapeutic intervention. We have developed a novel method to reconstitute V-ATPase into native lipid containing nanodiscs for biolayer interferometry. We demonstrate that the method can be used to determine binding constants and to study V-ATPase disassembly in real time.

Grant sponsor: NIH; Grant number: GM058600.

Correspondence to: Stephan Wilkens; Department of Biochemistry and Molecular Biology, SUNY Upstate Medical University, 750 East Adams Street, Syracuse, NY 13210. E-mail: wilkenss@upstate.edu

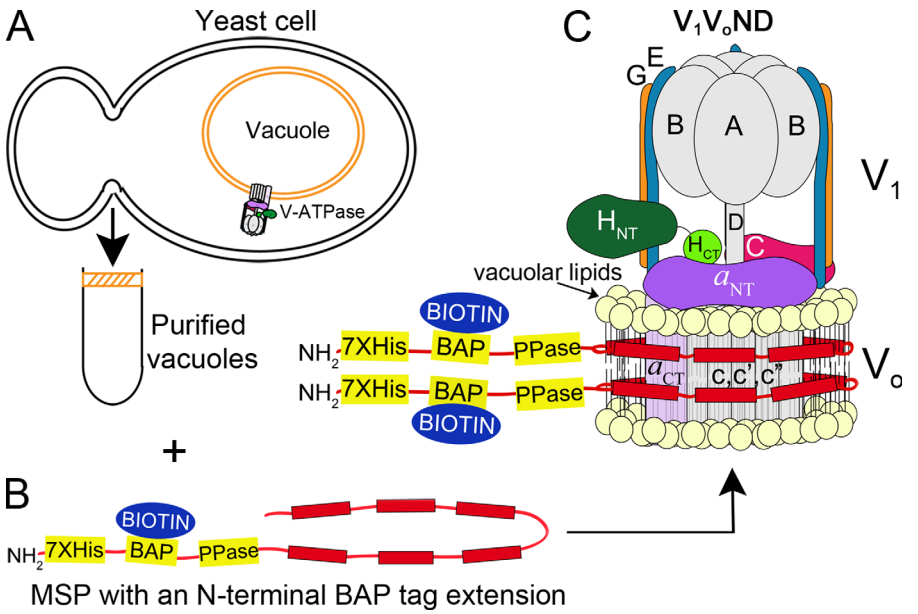

Figure 1. Purification and reconstitution strategy. (A) Yeast cells are lysed and vacuoles purified by flotation on a Ficoll gradient. (B) MSP with an N-terminal extension containing a BAP tag for *in vivo* biotinylation and a Prescission protease cleavage site (PPase) is expressed in *E. coli*. Vacuoles are detergent solubilized and total vacuolar membrane proteins are nanodisc-reconstituted using vacuolar lipids and biotinylated MSP. From this mixture of nanodisc-reconstituted membrane proteins, V-ATPase-containing nanodiscs are purified by affinity chromatography using a FLAG-tag at the G subunit N-terminus. (C) V-ATPase reconstituted in biotinylated and vacuolar lipid containing nanodiscs is schematically depicted as V_1V_0ND. V-ATPase is composed of a cytosolic V_1-ATPase sector and a membrane integral V_0 proton channel sector.

such as osteoporosis,[4] renal tubular acidosis,[5] deafness,[6] male infertility,[7] viral infection,[8] diabetes,[9] and cancer,[10] and it has been suggested that V-ATPase may represent a valuable drug target for the development of therapies against these diseases.[11,12]

V-ATPase is a membrane integral, multi-subunit protein complex composed of a cytosolic ATP hydrolyzing sector, V_1, and a membrane-integral ion translocating sector, V_0 (Fig. 1). V-ATPase is highly conserved from yeast to human and thanks to the relative ease of genetic manipulation, yeast has been a powerful model system to study the structure and mechanism of the eukaryotic enzyme. In yeast, V_1 is composed of subunits $A_3B_3(C)DE_3FG_3H$[13] and V_0 contains subunits a,c_8,c',c'',d,e,f.[14,15] V-ATPase belongs to the family of rotary motor enzymes that also includes F- and A-ATPase/synthase found in bacteria, mitochondria, chloroplasts and Archaea. ATP hydrolysis in V_1 is coupled to rotation of a membrane integral ring of c subunits ("proteolipid" ring, composed of c_8,c',c'') in V_0, which results in an uphill transport of protons across the membrane.[16] However, unlike F- and A-type motors, V-ATPase is regulated *in vivo* by a unique mechanism referred to as "reversible disassembly", a process first described in yeast[17] and insect.[18] Upon nutrient deprivation in yeast, for example, V_1 disengages from V_0 with concomitant silencing of the enzyme's ATPase and proton translocation activities. Reversible enzyme dissociation is conserved in higher organisms[19–23] and it has been proposed that the process provides a unique opportunity for therapeutic intervention by allowing for modulation of V-ATPase activity (rather than complete inhibition) in a tissue specific manner.[24] Reversible disassembly has been extensively studied in yeast[25] and insect[26] and it is known that the process requires an ATP hydrolysis competent enzyme[25,27] in addition to transient interaction with cellular effectors[28] and chaperones.[29] Understanding these interactions and their role in reversible disassembly would greatly benefit from a controlled *in vitro* system employing purified components. However, the limited stability of detergent solubilized V-ATPase and the difficulties with analyzing protein–protein interactions in presence of detergent have limited such studies thus far.

Here we have developed a method for reconstituting V-ATPase into lipid nanodiscs using native vacuolar lipids and membrane scaffold protein (MSP) engineered to contain an N-terminal biotin acceptor protein (BAP) tag for biotinylation in E. coli. We show that lipid nanodisc-reconstituted V_1V_0 (V_1V_0ND) is highly active and that the preparation can be immobilized on streptavidin-coated biosensors for binding studies using biolayer interferometry (BLI). We further demonstrate that the system can be used to study the kinetics of the interaction between V-ATPase and cellular factors known to bind to the enzyme and for monitoring the nucleotide-dependent dissociation of the complex in real time.

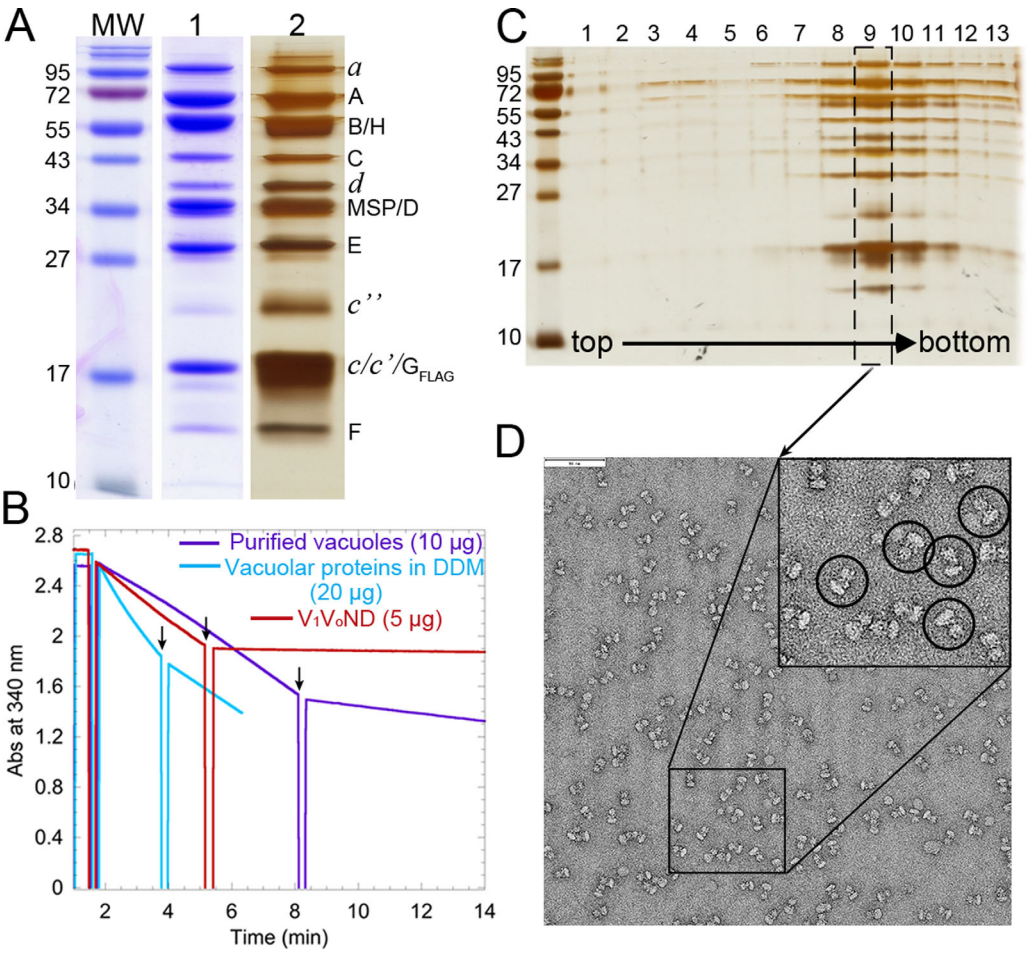

Figure 2. Characterization of V-ATPase in lipid nanodiscs. (A) SDS-PAGE of purified V_1V_0ND showing the subunits of the V-ATPase along with MSP. The three lanes show molecular weight markers (MW) and V_1V_0ND, both Coomassie blue (1) and silver stained (2). (B) Representative ATPase activity measurements using an ATP regenerating assay with 10 µg purified vacuoles (purple trace), 20 µg DDM solubilized vacuoles (blue trace), and 5 µg purified V_1V_0ND (red trace). The black arrows indicate points where 0.4 µ*M* ConA was added in each case. The change in absorbance measured as a function of time was used to calculate the specific activity before and after addition of ConA. (C) Silver stained SDS-PAGE of the fractions from the glycerol gradient. (D) Negative stain electron micrograph of purified V_1V_0ND (fraction 9 of the glycerol gradient in panel (C)), showing monodisperse and assembled enzyme complexes. A 2× enlargement of the boxed region is shown as an inset and single V_1V_0ND particles are highlighted by the black circles. Bar is 90 nm.

Results

Preparation and characterization of lipid nanodisc-reconstituted V-ATPase

We initially attempted to first affinity purify V-ATPase followed by nanodisc reconstitution using *E. coli* polar lipids as described for P-glycoprotein.[30] However, the tendency of the detergent solubilized enzyme to dissociate precluded this approach. We therefore developed a procedure that minimizes prolonged detergent exposure and allows for retention of native vacuolar lipids, some of which have been shown to be essential for enzyme function.[31] To that end, total vacuolar proteins are detergent solubilized, reconstituted into nanodiscs with native vacuolar lipids (without the addition of exogenous lipids) followed by affinity purification of nanodisc-reconstituted V_1V_0 (V_1V_0ND) (Fig. 1). The resulting V_1V_0ND preparation is highly purified, showing bands for all the V-ATPase subunits that can be resolved on SDS-PAGE gels as seen in earlier preparations of detergent solubilized enzyme[32] besides a band for MSP [Fig. 2(A)]. V_1V_0ND displays robust MgATPase activity of ~7.3 ± 0.3 U/mg (three independent purifications), 98% of which is inhibited by Concanamycin A [Fig. 2(B), red trace]. Concanamycin A (ConA) is a specific inhibitor of the V-ATPase that binds to V_0 and inhibits rotation of the proteolipid ring, in turn inhibiting ATPase activity in the coupled V_1.[33] The specific activity of purified vacuoles was ~2.9 ± 0.9 U/mg (nine independent purifications), consistent with previously published results.[34] Upon solubilization of vacuoles with dodecyl maltoside (DDM), the specific activity remained unchanged. However, while ~85% of the ATPase activity of

vacuoles was inhibited by ConA [Fig. 2(B), purple trace], inhibition of detergent-solubilized enzyme was only ~58% [Fig. 2(B), blue trace], suggesting that detergent causes partial uncoupling of the enzyme as has been described for the related F-ATPase.[35] Therefore, the virtually complete inhibition of V_1V_0ND's ATPase activity by ConA indicates tight coupling of ATPase and proton pumping activities in lipid nanodisc-reconstituted V_1V_0. To verify the structural integrity of purified V_1V_0ND, the preparation was subjected to glycerol gradient centrifugation followed by negative stain electron microscopy (EM). As can be seen from the silver stained SDS-PAGE gel of the glycerol gradient fractions, the majority of the preparation migrated in a single peak on the gradient with only trace amounts of free subunits in fractions near the top of the gradient [Fig. 2(C)]. Negative stain EM analysis of the peak fraction of the glycerol gradient shown in Figure 2(C) showed monodisperse particles with the characteristic dumbbell shape of V-ATPase complexes [Fig. 2(D)]. Taken together, reconstitution of V-ATPase into lipid nanodiscs using native vacuolar lipids allows purification of a stable, highly active, and monodisperse enzyme preparation suitable for structural and biophysical studies.

Biolayer interferometry of V_1V_0ND for analysis of protein binding

The MSP used for reconstitution of the V-ATPase into lipid nanodiscs contained an engineered N-terminal BAP tag for specific attachment of a single biotin during protein expression in E. coli (Fig. 1). Initial experiments revealed that the level of biotinylation of MSP was close to stoichiometric (Supporting Information Fig. S1), that the biotin tag in V_1V_0ND was accessible for binding to streptavidin-coated BLI sensors, and that a concentration of ~5 μg/mL V_1V_0ND produced sufficient BLI signal for subsequent binding or dissociation experiments (data not shown). As a proof-of-principle, we then tested binding of the well characterized V-ATPase inhibitor SidK to immobilized V_1V_0ND for determining kinetic constants of the interaction (Fig. 3). SidK is a ~60 kDa soluble polypeptide expressed by the pathogenic organism *Legionella pneumophilia* that specifically targets host cell V-ATPases to inhibit phagosome acidification and subsequent digestion of the bacterium. It was previously shown that SidK inhibits yeast V-ATPase by binding to the catalytic A subunit of the complex.[36] BLI sensors with immobilized V_1V_0ND were dipped in wells containing different concentrations of purified GST-tagged SidK. The SidK–V_1V_0ND interaction exhibited concentration dependence and the association and dissociation rates were used to estimate a K_d of the interaction of ~ 3.5 n*M* (Fig. 3). In another experiment, we tested binding of a monoclonal antibody directed against the catalytic A subunit of the enzyme and fitting of

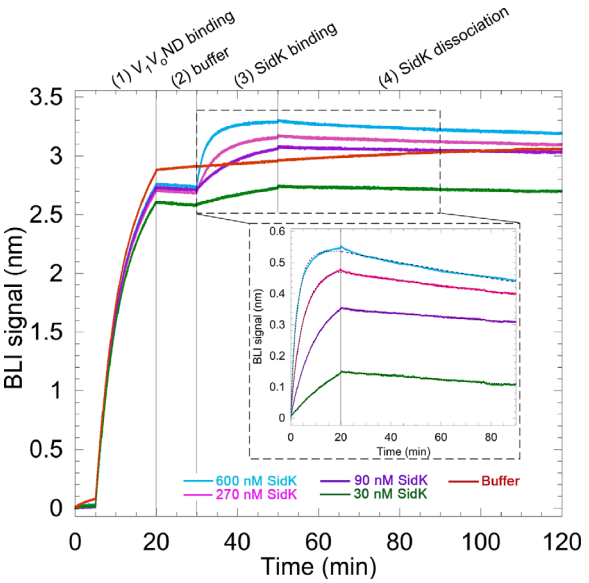

Figure 3. Biolayer interferometry with V_1V_0ND. 5 μg/mL of biotinylated V_1V_0ND was used to load streptavidin sensors (step 1) followed by dipping the sensors in buffer (step 2). The sensors were then dipped into wells containing either buffer, 30, 90, 270, or 600 n*M* of GST-tagged SidK to measure association rates (step 3). All the sensors were then dipped into buffer containing wells to measure dissociation rates (step 4). GST-SidK showed concentration dependent interaction with V_1V_0ND as evident from the association and dissociation phases (enlarged box). The signal obtained in buffer (red) was subtracted from the GST-SidK signal and the resultant curves were globally fit to a one site binding equation (black dotted traces). The on rate was found to be $1.25 \times 10^4 \pm 19$ s^{-1} and the off rate was $4.4 \times 10^{-5} \pm 9.7 \times 10^{-8}$ s^{-1}, resulting in a K_d of ~3.5 n*M*. Representative experiment from two repeats is shown.

the binding data revealed a tight interaction in the sub-n*M* range (Supporting Information Fig. S2). In summary, the binding experiments described above demonstrate that V-ATPase reconstituted into nanodiscs using native lipids and biotinylated MSP can be used for BLI to study the kinetics of inhibitor and antibody binding.

Dissociation of V_1 from V_o monitored by biolayer interferometry

As mentioned earlier, under conditions of starvation, V_1 dissociates from V_0, causing silencing of the enzymes ATPase and proton translocation activities. We used immobilized V_1V_0ND for BLI as an experimental setup to understand the kinetics of the dissociation of V_1 from V_0. From experiments with yeast vacuoles, it is known that V_1 can be released from membrane integral V_0 by treatment with chaotropic agents such as KNO_3 or KI in presence of MgATP.[37,38] To determine the rate of chaotrope-induced dissociation, BLI sensors with immobilized V_1V_0ND were dipped into wells containing KNO_3 with or without 1 m*M* MgATP (Fig. 4). Under these

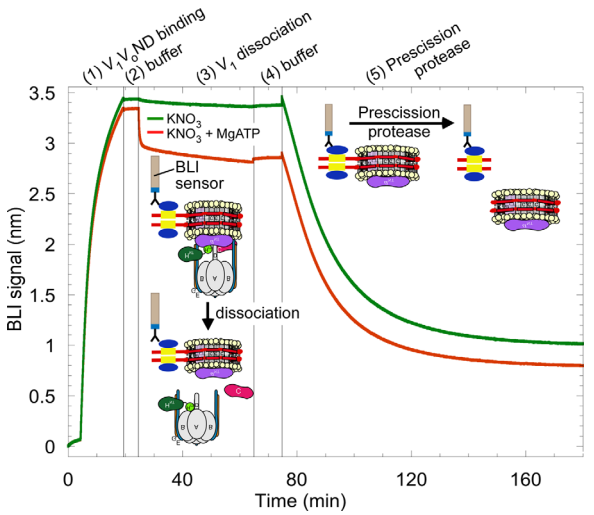

Figure 4. Biolayer interferometry to monitor the dissociation of V_1 from V_0 in real time. 5 μg/mL of biotinylated V_1V_0ND was used to load the streptavidin sensors (step 1) followed by dipping the sensors in buffer (step 2). One sensor was dipped in 300 m*M* KNO_3 (green trace) while the other sensor was dipped in 300 m*M* KNO_3 with 1 m*M* MgATP (red trace) (step 3). In the presence of both KNO_3 and MgATP, V_1 was released from V_0 as indicated by a fast drop in BLI signal (red trace, step 3). The sensors were then dipped in buffer (step 4). The remaining V_1V_0ND and V_0ND molecules on the sensors were then released by dipping the sensors in 0.2 U/μL of Prescission protease (step 5). The experiment has been illustrated using schematics of V_1V_0ND and its components. Representative experiment from two repeats is shown.

conditions, the BLI signal rapidly decreased but only when MgATP and the chaotrope were present together, consistent with the earlier experiments using yeast vacuoles.[37,38] Upon chaotrope treatment in presence of MgATP, the BLI signal decreased by only ~15%, an unexpected finding considering that the size of the V_1 sector (~600 kDa) is comparable to the size of V_0 in nanodiscs (~400 kDa without lipids). However, incomplete stripping of V_1 from V_0 had also been observed after chaotrope treatment of yeast vacuoles.[37,38] It is also possible that the majority of the BLI signal was due to the nanodisc bound V_0 as the method of detection could be more sensitive to the nanodiscs bound close to the sensor surface. As a control, chaotrope treated sensors were dipped into wells containing Prescission protease. The close to complete loss of signal due to proteolytic cleavage of the protease site engineered between the BAP tag and the N-terminus of MSP [Fig. 1(B)] confirmed that the majority of the initial BLI signal was due to specific binding of V_1V_0ND via biotinylated MSP (Fig. 4).

Of course, chaotrope induced dissociation is not physiological and to estimate the propensity of the enzyme to dissociate under more native conditions, we tested the effect of nucleotides and known V-ATPase inhibitors on the dissociation of V_1 from V_0 (Fig. 5). To that purpose, BLI sensors with immobilized V_1V_0ND were dipped in wells containing MgATP (Fig. 5, pink trace), MgATP with ConA (V_0 inhibitor) (Fig. 5, orange trace), MgATP with N-ethylmaleimide (NEM; V_1 inhibitor), which covalently modifies an essential cysteine in the P-loops of the catalytic A subunits, thereby preventing substrate binding to active sites[39] (Fig. 5, red trace), MgAMPPNP, which is a non-hydrolyzable substrate analog of MgATP (V_1 inhibitor) (Fig. 5, blue trace) and MgATP with KNO_3 as a control (Fig. 5, purple trace). We found that V_1 was released from V_0 at a slow rate ($k_{off} \sim 1 \times 10^{-3}$ s^{-1}) in the presence of MgATP, suggesting that rotary catalysis destabilizes the V_1/V_0 interface. Dissociation of V_1 from V_0 in the presence of MgATP has also been observed for the purified detergent solubilized insect V-ATPase,[27] suggesting that destabilization of the V_1/V_0 interface due to ATP hydrolysis is a conserved feature of the enzyme. Consistent with earlier findings that V-

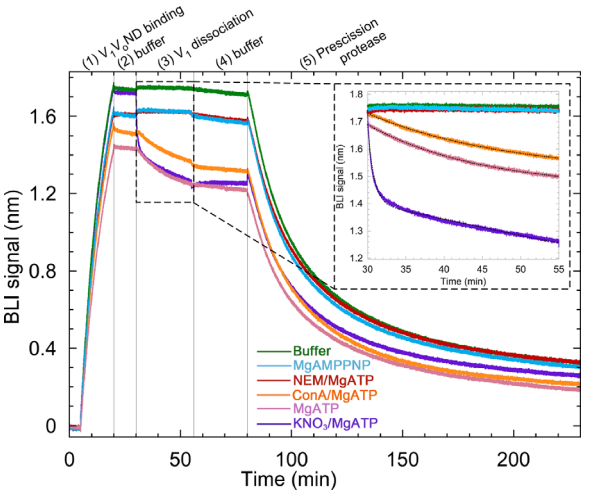

Figure 5. Effect of nucleotides and inhibitors on the dissociation of V_1 from V_0. V_1V_0ND immobilized on streptavidin sensors (step 1) was dipped into buffer (step 2), and then into wells containing either buffer, 1 m*M* MgATP, 1 m*M* MgAMPPNP, 2 m*M* NEM/1 m*M* MgATP, 0.2 μM Concanamycin A/1 m*M* MgATP, or 300 m*M* KNO_3/1 m*M* MgATP (step 3) followed by buffer (step 4). Following dissociation of V_1 from V_0 in step 3, the remaining V_1V_0ND or V_0ND was released from the sensors using 0.2 U/μL of Prescission protease (step 5). Inset: Enlarged view of the dissociation of V_1 from V_0 (step 3). In the presence of MgATP and MgATP/ConA (pink and orange traces, respectively), V_1 is released from V_0 at a slow rate. The two curves were fit to the equation for a single exponential decay (black dotted trace) and the off rates were found to be $1 \times 10^{-3} \pm 3.3 \times 10^{-6}$ s^{-1} in MgATP and $9 \times 10^{-4} \pm 3.3 \times 10^{-6}$ s^{-1} in ConA/MgATP. In the presence of KNO_3/MgATP, V_1 was released from V_0 with an initial fast rate of $2.1 \times 10^{-2} \pm 1 \times 10^{-6}$ s^{-1} followed by a slow off rate of $7.5 \times 10^{-5} \pm 1.6 \times 10^{-7}$ s^{-1}. In the presence of buffer (green), MgAMPPNP (blue) and NEM/MgATP (red), V_1 remains associated with V_0 over the duration of the experiment. Representative experiment from two repeats is shown.

ATPase must be ATP hydrolysis-competent for in vivo dissociation to occur,[25,40] we observed that inhibition of V_1 by MgAMPPNP or NEM prevented dissociation (Fig. 5). Interestingly, release of V_1 from V_0 under conditions of ATP hydrolysis did not appear to be impaired in presence of ConA, an observation that seems inconsistent with the fact that V_1V_0ND's ATPase activity is close to zero in presence of the inhibitor [Fig. 2(B)].

Taken together, the results show that BLI of immobilized V_1V_0ND can be used to monitor the dissociation of the complex in real time and while the observed rate of dissociation is significantly lower than the rate observed in live yeast,[25] above experiments indicate that V_1V_0ND is disassembly competent during catalytic turnover.

Discussion

Biophysical characterization of membrane proteins and membrane protein–protein interaction is challenging due to the presence of detergents that are required for keeping membrane proteins water soluble. Detergents are known to destabilize multisubunit membrane protein complexes[35,41] and the light scattering from detergent micelles can interfere with binding assays that depend on optical detection methods. The results summarized above indicate that there are two major advantages of using the "nanodisc-reconstitution before purification" strategy. First, the lipids used for the process of reconstitution were derived directly from yeast vacuoles and therefore represent the native environment of the enzyme, an important aspect as it has been shown that *in vivo* V-ATPase activity depends on low abundance, long chain fatty acid sphingolipids.[31] Second, V-ATPase is held together by multiple low-affinity protein-protein interactions for efficient enzyme regulation by reversible disassembly.[42] These low-affinity interactions are susceptible to breakage when exposed to detergent for long periods of time. Multiple attempts were made to first extract and purify the V-ATPase from pelleted membranes followed by reconstitution into E. coli lipid-containing nanodiscs as described for the enzyme's V_0 membrane sector.[43] However, likely due to the prolonged exposure to detergent required for purifying the complex, the resultant preparation showed a significant fraction of disassembled V_1 and V_0 particles with little or no measurable ATPase activity (data not shown). Using the "nanodisc-reconstitution before purification" strategy to obtain V_1V_0ND, we found that the resulting preparation consisted of close to completely assembled V-ATPase with high specific ATPase activity. The ATPase activity was 98% inhibited by Concanamycin A, suggesting tight coupling between V_1V_0ND's V_1 and V_0 sectors.

For immobilization on streptavidin-coated BLI sensors, we engineered a BAP tag at the N-terminus of MSP for site directed biotinylation during expression in E. coli. The high affinity of the streptavidin-biotin interaction allows immobilization of V_1V_0ND at a relatively low concentration with little risk of nonspecific binding. We first showed that our method can be used successfully to study the kinetics of interaction of the V-ATPase with binding partners such as an anti-subunit A monoclonal antibody and the pathogen derived inhibitor, SidK. Both examples allowed an estimate of the K_ds of the interactions ranging from the sub-nM (anti-A mAb) to the low nM (SidK) range. In addition, we showed that the dissociation of V_1 from V_0 under different conditions could be monitored in real time. The data indicate that ATP hydrolysis is required for disassembly to occur, consistent with *in vivo* and *in vitro* experiments conducted with yeast cells[25] and detergent solubilized insect V-ATPase,[27] respectively. However, the observation that the V_0 specific inhibitor ConA did not prevent or slow down disassembly was surprising, but it is possible that residual turnover and/or the conformational changes induced by rapid binding and release of MgATP are sufficient to destabilize the complex. It should be noted that the rate of V_1V_0 disassembly upon glucose withdrawal in live yeast occurs within minutes and is therefore significantly faster than the rate observed here. Thus, while the experiment shows that MgATP hydrolyzing V-ATPase has the propensity to dissociate, additional events induced by, for example, nutrient withdrawal are required to accelerate the process. The experimental setup developed here will allow for a systematic analysis of the cellular factors that may be involved in promoting or impeding the disassembly process in vivo such as phosphorylation,[26] variations in pH[44] and the interaction with mTORC,[22] phosphoinositides[45] or glycolytic enzymes.[28]

Conclusion and Future Perspective

We have developed a procedure to reconstitute yeast V-ATPase into native lipid containing nanodiscs for binding and dissociation assays using biolayer interferometry. Recent progress with the structure determination of the assembled V-ATPase[15] along with those of the disassembled and silenced V_1[46] and V_0[43,47] suggest that following disassembly, there is a mismatch in the subunit conformations between V_1 and V_0 that may act to prevent spontaneous reassembly under conditions when enzyme activity is not desired.[43,46] To overcome the kinetic barriers for reassembly created by the conformational mismatch, subunit rearrangements at the V_1/V_0 interface facilitated by effector and chaperone proteins such as the RAVE complex[48] are required. The here developed tool of immobilizing V_1V_0ND for BLI can be used to study the function of these effector and chaperone proteins in the (re)assembly process. The method can also be extended to the discovery of small

molecules that will modulate enzyme assembly, a strategy that may ultimately lead to the development of therapies designed to overcome aberrant V-ATPase activity in human disease.

Materials and Methods

Materials

The plasmid encoding 6XHis-tagged membrane scaffold protein, pMSP1E3D1, was a gift from Dr. Stephen Sligar (Addgene plasmid # 20066).[49] Molecular biology reagents were purchased from Takara Bio Inc. Zymolyase 100T was from amsbio. An N-terminal extension of MSP encoding the 7XHis tag, BAP tag and Prescission protease cleavage site was synthesized and subcloned into the pET28a vector (pMSP1E3D1) by Bio Basic Inc., resulting in plasmid pHBPMSP1E3D1. All other reagents were of analytical grade.

Strains

A yeast strain deleted for the VMA10 gene (subunit G), BY4741 vma10Δ:: KanMX was a kind gift from Dr. Patricia Kane, SUNY Upstate Medical University. The 3′ and 5′ UTR regions of VMA10 along with the KanMX selection marker was amplified from genomic DNA using the following primers: Vma10-delKanfwd: 5′ gcc aca ccc ttc cct att aac tgg act cc tat tcc agc tca tc 3′ and Vma10delKanrev: 5′ ggc tga atg gat aaa gcg aga gtc gta aag acc gaa tgc aat gtc 3′. The PCR product was gel purified and transformed into a wild-type yeast strain SF838-5Aα[50] for homologous recombination. Transformants were selected based on their resistance to G418 and their inability to grow on pH 7.5 and Ca^{2+}. Deletion of the VMA10 gene was confirmed by DNA sequencing. For affinity purification of V_1V_0ND, SF838-5Aα vma10Δ::KanMX was transformed with a pRS315 plasmid encoding the G subunit with an N-terminal FLAG-tag.[51]

Purification of biotinylated MSP

A plasmid encoding the BirA gene for *in vivo* biotinylation of the BAP tag (pBirAcm[52]) was a kind gift from Dr. Thomas Duncan, SUNY Upstate Medical University. E. coli strain BL21 (DE3) was co-transformed with pHBPMSP1E3D1 and pBirAcm. Cells were grown in rich broth supplemented with 0.1 m*M* D-biotin, 34 μg/mL chloramphenicol and 30 μg/mL kanamycin at 37°C to an OD_{595} of ∼0.5 followed by induction with 0.5 m*M* IPTG at 37°C for 3–4 h. Biotinylated MSP was purified as described.[43] The extent of biotinylation of MSP was estimated by performing pull down assays with streptactin beads as follows. MSP eluted from the Ni column was diluted 1:2 and 1:3 in streptactin buffer (15 m*M* Tris, pH 7.8, 150 m*M* NaCl, 0.5 m*M* EDTA) and incubated with 100 μL streptactin beads at 4°C for 1 h. The beads were washed for 1 h at 4°C in streptactin buffer, boiled in cracking buffer for 10 min and the beads, supernatant and wash were resolved using SDS-PAGE. 100 μL of streptactin buffer served as a control.

Isolation of vacuoles

Vacuoles were isolated by flotation on Ficoll density gradients as described with the following modifications.[53] Briefly, yeast strain SF838-5Aα vma10Δ transformed with pRS315 encoding FLAG tagged G subunit[51] was grown to an OD_{595} of ∼1.0 in YPD, pH 5 media and harvested by centrifugation at 5,000×g for 30 min. Cells from 12 l of culture were washed and resuspended in 100 mL of 1.2*M* sorbitol supplemented with ∼15 mg of zymolyase. Spheroplasts were recovered in 100 mL of 2× YPD and 100 mL of 2.4*M* sorbitol followed by resuspension in buffer A (10 m*M* MES–Tris pH 6.9, 0.1 m*M* $MgCl_2$, and 12% Ficoll 400) supplemented with 1 m*M* PMSF and 2 μg/mL each of leupeptin, pepstatin, and chymostatin. The suspension was homogenized in a Dounce homogenizer using ten strokes and centrifuged for 40 min at 71,000×g. Vacuole wafers on top of the gradient were resuspended in buffer B containing 8% Ficoll 400, homogenized and centrifuged for 40 min at 71,000×g. Wafers were collected and resuspended in 1.5 m*M* Mes–Tris, pH 7.0, 4.8% glycerol, 1 m*M* BME. Vacuoles were analyzed for Concanamycin A sensitive ATPase activity using an ATP regenerating assay[46] and protein concentration was determined with a modified BCA assay.[54] Vacuoles were frozen in liquid nitrogen until further use.

Extraction of V-ATPase and reconstitution into lipid nanodiscs

Typically three batches of vacuoles (12 liters each) were thawed, combined and supplemented with 1 m*M* PMSF and 2 μg/mL each of leupeptin, pepstatin, and chymostatin. 1.2 mg of *n*-dodecyl β-D-maltopyranoside (DDM) per 1 mg of vacuolar membrane protein was added to the vacuoles and the mixture was rotated for 1 h at 4°C. Detergent solubilized vacuoles were centrifuged at 100,000×g for 15 min. The pellet was discarded and the supernatant was used for reconstitution into lipid nanodiscs. To the detergent solubilized vacuole sample containing vacuolar lipids, purified biotinylated MSP was added in a molar ratio of 1:50 (vacuolar protein: biotinylated MSP) and the mixture was rotated at 4°C for 1 h followed by the addition of 1.5 g of activated bio-beads and rotation of the sample at 4°C for 2 h to remove detergent. V-ATPase containing lipid nanodiscs were then separated by anti-FLAG affinity chromatography (Fig. 1). The FLAG column eluate was concentrated using a Vivaspin concentrator (100,000 MWCO) and subjected to a 50–20% glycerol gradient

density centrifugation as described.[53] 400 μL fractions were collected from top to bottom and analyzed by SDS-PAGE. For negative stain electron microscopy, 5 μL of V_1V_0ND (1:10 diluted from fraction 9 of the density gradient) was applied to glow-discharged carbon-coated copper grids and stained with 1% uranyl formate. Micrographs were collected on a JEOL JEM-2100 at a magnification of 60,000× and a defocus of −1.5 μm.

Purification of GST-SidK

The plasmid for overexpression of GST-tagged SidK (pzl797) was a kind gift from Zhao-Qing Luo, Purdue University.[36] E. coli Rosetta2 cells (Novagen) were transformed with pzl797 and the cells were grown in rich broth supplemented with 34 μg/mL Ampicillin and 34 μg/mL Chloramphenicol. Cells were induced with 0.5 m*M* IPTG at an OD_{595} of ∼0.5 and grown for 6 h at 25°C. Cells were pelleted by centrifugation at 3000×g, resuspended in GST buffer (10 m*M* Tris pH 7.8, 150 m*M* NaCl, 0.5 m*M* EDTA, 1 m*M* DTT) and stored at −20°C until use. Cells were lysed by sonication in the presence of 20 μg/mL DNase, 1 mg/mL lysozyme and 1 m*M* PMSF. Lysed cells were centrifuged at 13,000×g for 40 min and the supernatant was subjected to affinity chromatography using a pre-equilibrated GST column. The column was washed with ten column volumes of GST buffer and eluted in ten 2 mL fractions using 10 m*M* reduced glutathione. To improve purity, eluted GST-SidK was subjected to size exclusion chromatography using a Superdex 200 1.6 cm × 50 cm column attached to an Äkta FPLC (GE Healthcare). The peak fractions were pooled, analyzed by SDS-PAGE and used for biolayer interferometry.

Biolayer interferometry

An Octet-RED system with streptavidin-coated sensors (FortéBio, SA biosensors, catalog number 18-5019) were used for biolayer interferometry, a technique similar to surface plasmon resonance.[55] In all BLI experiments described, the buffer used was 20 m*M* Tris, pH 7.4 with 150 m*M* NaCl, 0.5 m*M* EDTA, 1 m*M* β mercaptoethanol and 0.5 mg/mL BSA. All steps were conducted at 22°C with each biosensor stirred in 0.2 mL of sample at 1000 rpm and a standard measurement rate of 5 s^{-1}. In each case, the biosensors were pre-wetted in BLI buffer for 10 min and then dipped in wells containing 5 μg/mL V_1V_0ND. Control experiments were performed to show that the buffer components did not interact with the streptavidin sensors. Details of individual BLI experiments are given in their respective figure legends. FortéBio's data analysis software (version 6.4) was used for subtraction of reference sensors, Savitsky–Golay filtering and global or local fitting of the kinetic rates where applicable.

Acknowledgments

We thank Dr. Patricia Kane for yeast strains and reagents, Dr. Thomas Duncan for help with biolayer interferometry and Dr. Rebecca Oot, Mr. Sergio Couoh-Cardel, and Mr. Nicholas Stam for helpful discussions and for critically reading the manuscript.

Conflict of Interest

The authors declare that they have no conflicts of interest with the contents of this article.

References

1. Forgac M (2007) Vacuolar ATPases: rotary proton pumps in physiology and pathophysiology. Nat Rev Mol Cell Biol 8:917–929.
2. Inoue H, Noumi T, Nagata M, Murakami H, Kanazawa H (1999) Targeted disruption of the gene encoding the proteolipid subunit of mouse vacuolar H(+)-ATPase leads to early embryonic lethality. Biochim Biophys Acta 1413:130–138.
3. Sun-Wada G, Murata Y, Yamamoto A, Kanazawa H, Wada Y, Futai M (2000) Acidic endomembrane organelles are required for mouse postimplantation development. Dev Biol 228:315–325.
4. Thudium CS,VKJ, Karsdal MA, Henriksen K (2012) Disruption of the V-ATPase functionality as a way to uncouple bone formation and resorption—a novel target for treatment of osteoporosis. Curr Prot Pept Sci 13:141–151.
5. Smith AN, Skaug J, Choate KA, Nayir A, Bakkaloglu A, Ozen S, Hulton SA, Sanjad SA, Al-Sabban EA, Lifton RP, Scherer SW, Karet FE (2000) Mutations in ATP6N1B, encoding a new kidney vacuolar proton pump 116-kD subunit, cause recessive distal renal tubular acidosis with preserved hearing. Nat Genet 26: 71–75.
6. Karet FE, Finberg KE, Nelson RD, Nayir A, Mocan H, Sanjad SA, Rodriguez-Soriano J, Santos F, Cremers CW, Di Pietro A, Hoffbrand BI, Winiarski J, Bakkaloglu A, Ozen S, Dusunsel R, Goodyer P, Hulton SA, Wu DK, Skvorak AB, Morton CC, Cunningham MJ, Jha V, Lifton RP (1999) Mutations in the gene encoding B1 subunit of H+-ATPase cause renal tubular acidosis with sensorineural deafness. Nature Genet 21: 84–90.
7. Breton S, Smith PJ, Lui B, Brown D (1996) Acidification of the male reproductive tract by a proton pumping (H+)-ATPase. Nat Med 2:470–472.
8. Lu X, Yu H, Liu SH, Brodsky FM, Peterlin BM (1998) Interactions between HIV1 Nef and vacuolar ATPase facilitate the internalization of CD4. Immunity 8:647–656.
9. Sun-Wada GH, Toyomura T, Murata Y, Yamamoto A, Futai M, Wada Y (2006) The a3 isoform of V-ATPase regulates insulin secretion from pancreatic β-cells. J Cell Sci 119:4531–4540.
10. Sennoune SR, Bakunts K, Martínez GM, Chua-Tuan JL, Kebir Y, Attaya MN, Martínez-Zaguilán R (2004) Vacuolar H+-ATPase in human breast cancer cells with distinct metastatic potential: distribution and functional activity. Am J Physiol Cell Physiol 286: 1443–1452.
11. Fais S, De Milito A, You H, Qin W (2007) Targeting vacuolar H+-ATPases as a new strategy against cancer. Cancer Res 67:10627–10630.

12. Kartner N, Manolson MF (2014) Novel techniques in the development of osteoporosis drug therapy: the osteoclast ruffled-border vacuolar H+-ATPase as an emerging target. Expert Opin Drug Discov 9:505–522.
13. Kitagawa N, Mazon H, Heck AJ, Wilkens S (2008) Stoichiometry of the peripheral stalk subunits E and G of yeast V1-ATPase determined by mass spectrometry. J Biol Chem 283:3329–3337.
14. Powell B, Graham LA, Stevens TH (2000) Molecular characterization of the yeast vacuolar H+-ATPase proton pore. J Biol Chem 275:23654–23660.
15. Zhao J, Benlekbir S, Rubinstein JL (2015) Electron cryomicroscopy observation of rotational states in a eukaryotic V-ATPase. Nature 521:241–245.
16. Stewart AG, Sobti M, Harvey RP, Stock D (2013) Rotary ATPases: models, machine elements and technical specifications. Bioarchitecture 3:2–12.
17. Kane PM (1995) Disassembly and reassembly of the yeast vacuolar H(+)-ATPase *in vivo*. J Biol Chem 270: 17025–17032.
18. Sumner JP, Dow JA, Earley FG, Klein U, Jager D, Wieczorek H (1995) Regulation of plasma membrane V-ATPase activity by dissociation of peripheral subunits. J Biol Chem 270:5649–5653.
19. Trombetta ES, Ebersold M, Garrett W, Pypaert M, Mellman I (2003) Activation of lysosomal function during dendritic cell maturation. Science 299:1400–1403.
20. Lafourcade C, Sobo K, Kieffer-Jaquinod S, Garin J, van der Goot FG (2008) Regulation of the V-ATPase along the endocytic pathway occurs through reversible subunit association and membrane localization. PLoS One 3:e2758.
21. Sautin YY, Lu M, Gaugler A, Zhang L, Gluck SL (2005) Phosphatidylinositol 3-kinase-mediated effects of glucose on vacuolar H+-ATPase assembly, translocation, and acidification of intracellular compartments in renal epithelial cells. Mol Cell Biol 25:575–589.
22. Zoncu R, Bar-Peled L, Efeyan A, Wang S, Sancak Y, Sabatini DM (2011) mTORC1 senses lysosomal amino acids through an inside-out mechanism that requires the vacuolar H(+)-ATPase. Science 334:678–683.
23. Stransky LA, Forgac M (2015) Amino acid availability modulates vacuolar H+-ATPase assembly. J Biol Chem 290:27360–27369.
24. Kane PM (2012) Targeting reversible disassembly as a mechanism of controlling V-ATPase activity. Curr Prot Pept Sci 13:117–123.
25. Parra KJ, Kane PM (1998) Reversible association between the V1 and V0 domains of yeast vacuolar H+-ATPase is an unconventional glucose-induced effect. Mol Cell Biol 18:7064–7074.
26. Voss M, Vitavska O, Walz B, Wieczorek H, Baumann O (2007) Stimulus-induced phosphorylation of vacuolar H(+)-ATPase by protein kinase A. J Biol Chem 282: 33735–33742.
27. Huss M, Wieczorek H (2007) Influence of ATP and ADP on dissociation of the V-ATPase into its V(1) and V(O) complexes. FEBS Lett 581:5566–5572.
28. Lu M, Ammar D, Ives H, Albrecht F, Gluck SL (2007) Physical interaction between aldolase and vacuolar H+-ATPase is essential for the assembly and activity of the proton pump. J Biol Chem 282:24495–24503.
29. Smardon AM, Nasab ND, Tarsio M, Diakov TT, Kane PM (2015) Molecular interactions and cellular itinerary of the yeast RAVE (Regulator of the H+-ATPase of Vacuolar and Endosomal Membranes) complex. J Biol Chem 290:27511–27523.
30. Ritchie TK, Kwon H, Atkins WM (2011) Conformational analysis of human ATP-binding cassette transporter ABCB1 in lipid nanodiscs and inhibition by the antibodies MRK16 and UIC2. J Biol Chem 286:39489–39496.
31. Finnigan GC, Ryan M, Stevens TH (2011) A genome-wide enhancer screen implicates sphingolipid composition in vacuolar ATPase function in *Saccharomyces cerevisiae*. Genetics 187:771–783.
32. Zhang Z, Zheng Y, Mazon H, Milgrom E, Kitagawa N, Kish-Trier E, Heck AJ, Kane PM, Wilkens S (2008) Structure of the yeast vacuolar ATPase. J Biol Chem 283:35983–35995.
33. Huss M, Ingenhorst G, Konig S, Gassel M, Drose S, Zeeck A, Altendorf K, Wieczorek H (2002) Concanamycin A, the specific inhibitor of V-ATPases, binds to the V(o) subunit c. J Biol Chem 277:40544–40548.
34. Charsky CM, Schumann NJ, Kane PM (2000) Mutational analysis of subunit G (Vma10p) of the yeast vacuolar H+-ATPase. J Biol Chem 275:37232–37239.
35. Tsunoda SP, Aggeler R, Noji H, Kinosita K, Jr., Yoshida M, Capaldi RA (2000) Observations of rotation within the F(o)F(1)-ATP synthase: deciding between rotation of the F(o)c subunit ring and artifact. FEBS Lett 470:244–248.
36. Xu L, Shen X, Bryan A, Banga S, Swanson MS, Luo ZQ (2010) Inhibition of host vacuolar H+-ATPase activity by a *Legionella pneumophila* effector. PLoS Pathog 6:e1000822.
37. Parra KJ, Kane PM (1996) Wild-type and mutant vacuolar membranes support pH-dependent reassembly of the yeast vacuolar H+-ATPase *in vitro*. J Biol Chem 271:19592–19598.
38. Kane PM, Yamashiro CT, Stevens TH (1989) Biochemical characterization of the yeast vacuolar H(+)-ATPase. J Biol Chem 264:19236–19244.
39. Feng Y, Forgac M (1992) Cysteine 254 of the 73-kDa A subunit is responsible for inhibition of the coated vesicle (H+)-ATPase upon modification by sulfhydryl reagents. J Biol Chem 267:5817–5822.
40. MacLeod KJ, Vasilyeva E, Baleja JD, Forgac M (1998) Mutational analysis of the nucleotide binding sites of the yeast vacuolar proton-translocating ATPase. J Biol Chem 273:150–156.
41. Yang Z, Wang C, Zhou Q, An J, Hildebrandt E, Aleksandrov LA, Kappes JC, DeLucas LJ, Riordan JR, Urbatsch IL, Hunt JF, Brouillette CG (2014) Membrane protein stability can be compromised by detergent interactions with the extramembranous soluble domains. Protein Sci 23:769–789.
42. Oot RA, Wilkens S (2012) Subunit interactions at the V1–Vo interface in yeast vacuolar ATPase. J Biol Chem 287:13396–13406.
43. Stam NJ, Wilkens S (2016) Structure of nanodisc reconstituted vacuolar ATPase proton channel: definition of the interaction of rotor and stator and implications for enzyme regulation by reversible dissociation. J Biol Chem.
44. Dechant R, Binda M, Lee SS, Pelet S, Winderickx J, Peter M (2010) Cytosolic pH is a second messenger for glucose and regulates the PKA pathway through V-ATPase. EMBO J 29:2515–2526.
45. Li SC, Diakov TT, Xu T, Tarsio M, Zhu W, Couoh-Cardel S, Weisman LS, Kane PM (2014) The signaling lipid PI(3,5)P(2) stabilizes V(1)-V(o) sector interactions and activates the V-ATPase. Mol Biol Cell 25:1251–1262.
46. Oot RA, Kane PM, Berry EA, Wilkens S (2016) Crystal structure of yeast V1-ATPase in the autoinhibited state. EMBO J 35:1694–1706.

47. Mazhab-Jafari MT, Rohou A, Schmidt C, Bueler SA, Benlekbir S, Robinson CV, Rubinstein JL (2016) Atomic model for the membrane-embedded VO motor of a eukaryotic V-ATPase. Nature 539:118–122.
48. Smardon AM, Tarsio M, Kane PM (2002) The RAVE complex is essential for stable assembly of the yeast V-ATPase. J Biol Chem 277:13831–13839.
49. Denisov IG, Baas BJ, Grinkova YV, Sligar SG (2007) Cooperativity in cytochrome P450 3A4: linkages in substrate binding, spin state, uncoupling, and product formation. J Biol Chem 282:7066–7076.
50. Stevens TH, Rothman JH, Payne GS, Schekman R (1986) Gene dosage-dependent secretion of yeast vacuolar carboxypeptidase Y. J Cell Biol 102:1551–1557.
51. Zhang Z, Charsky C, Kane PM, Wilkens S (2003) Yeast V1-ATPase: affinity purification and structural features by electron microscopy. J Biol Chem 278:47299–47306.
52. Shah NB, Hutcheon ML, Haarer BK, Duncan TM (2013) F1-ATPase of *Escherichia coli*: the ϵ- inhibited state forms after ATP hydrolysis, is distinct from the ADP-inhibited state, and responds dynamically to catalytic site ligands. J Biol Chem 288: 9383–9395.
53. Uchida E, Ohsumi Y, Anraku Y (1985) Purification and properties of H+-translocating, Mg^{2+}-adenosine triphosphatase from vacuolar membranes of *Saccharomyces cerevisiae*. J Biol Chem 260:1090–1095.
54. Couoh-Cardel S, Milgrom E, Wilkens S (2015) Affinity purification and structural features of the yeast vacuolar ATPase Vo membrane sector. J Biol Chem 290: 27959–27971.
55. Shah NB, Duncan TM (2014) Bio-layer interferometry for measuring kinetics of protein–protein interactions and allosteric ligand effects. J Vis Exp 84:e51383.